Available online at www.sciencedirect.com
ScienceDirect
Inorganica Chimica Acta 360 (2007) 2623–2630
Inorganica Chimica Acta
www.elsevier.com/locate/ica

Synthesis of amidate-hanging platinum mononuclear complexes by base hydrolysis of nitrile complexes

Kazuhiro Uemura [1], Kana Yamasaki, Kôichi Fukui [2], Kazuko Matsumoto *

Department of Chemistry, School of Science and Engineering, Waseda University, 3-4-1, Ohkubo, Shinjuku, Tokyo 169-8555, Japan

Received 29 October 2006; received in revised form 23 December 2006; accepted 28 December 2006
Available online 9 January 2007

Abstract

The "amidate-hanging" Pt mononuclear complexes, which can easily bind a second metal ion with the non-coordinated oxygen atoms in the amidate moieties, have been synthesized and characterized by ^{1}H NMR, MS, IR spectroscopy, and single crystal X-ray analysis. Five new complexes with various amidate ligands and co-ligands, *cis*-$[Pt(PVM)_2(en)] \cdot 4H_2O$ (**1**, PVM = pivaloamidate, en = ethylenediamine), *cis*-$[Pt(PVM)_2(NH_2CH_3)_2] \cdot H_2O$ (**2**), *cis*-$[Pt(PVM)_2(NH_2{}^tBu)_2]$ (**3**), *cis*-$[Pt(TCM)_2(NH_3)_2]$ (**4**, TCM = trichloroacetamidate), and *cis*-$[Pt(BZM)_2(NH_3)_2]$ (**5**, BZM = benzamidate), were successfully synthesized by direct base hydrolysis of the corresponding Pt nitrile complexes, *cis*-$[Pt(NCR)_2(Am)_2]^{2+}$ (**P1**, **P2**, **P3**, and **P5**) (NCR = nitrile, Am = amine). These nitrile complexes were obtained by introducing nitriles into the Pt aqua complexes, *cis*-$[Pt(OH_2)_2(Am)_2](ClO_4)_2$, whereas introduction of trichloronitrile into $[Pt(OH_2)_2(NH_3)_2](ClO_4)_2$ induced more facilitated water nucleophilic attack to afford $[Pt(TCM)(NH(C{=}OH)CCl_3)(NH_3)_2](ClO_4)$ (**P4**). The base treatments of the precursor complexes (**P1**–**5**) lead to produce "amidate-hanging" Pt mononuclear complexes (**1**–**5**) without geometry isomerization. The ^{195}Pt chemical shifts for **1**–**5** exhibit subtle differences of the Pt electron densities among them.

Keywords: Platinum complexes; Amidate; Nitrile; Base hydrolysis; Crystal structures

1. Introduction

The occupied dz^2 orbital in the d^8 transition metal ion with square-planar coordination geometry can act as a donor to another metal ion (M) to form a dative $Pt(d^8) \rightarrow M$ bond, where the Pt dz^2 orbital is stabilized by overlap with the dz^2 orbital on M [1–3]. By utilizing such dative bonds, a large number of amidate-bridged Pt–M dinuclear and Pt–M–Pt trinuclear complexes of the formula $[(Am)_2Pt\text{-}M(Amid)_2]^{n+}$ and $[(Am)_2Pt(Amid)_2M(Amid)_2Pt(Am)_2]^{m+}$ (Amid = amidate, Am = amine) have been synthesized and characterized up to date [4–10]. Such hetero-nuclear complexes have been expected for the unique oxidation states and redox properties due to the metal–metal interaction. For example, our previously reported hetero-nuclear 1-D chain $(\{[PtRh(PVM)_2(NH_3)_2Cl_{2.5}]_2[Pt_2(PVM)_2(NH_3)_4]_2(PF_6)_6 \cdot 2MeOH \cdot 2H_2O\}_n)$, which comprises amidate-bridged Pt–Rh and Pt–Pt dinuclear complexes, showed the unprecedented phenomena that an unpaired electron hops among Rh atoms through the linear Pt units [11,12].

In order for rational synthesis of Pt and hetero-metal multinuclear linear complexes, "amidate-hanging" Pt mononuclear complexes $[Pt(Amid)_2(Am)_2]$ are suitable starting materials, since they can easily bind a second metal ion with the non-coordinated oxygen atoms in the amidate moieties (Scheme 1) [7,13]. Such complexes were prepared by utilizing the direct base hydrolysis of the corresponding *cis* Pt nitrile complexes [14–20]. In the procedure, no geometry isomerization took place during the hydrolysis,

* Corresponding author. Present address: 3-9-12-105, Daizawa, Setagaya-ku, Tokyo 155-0032, Japan. Tel./fax: +81 3 3413 5352.
E-mail address: kmatsu@yf6.so-net.ne.jp (K. Matsumoto).
[1] Present address: Environmental Science and Engineering, Graduate School of Science and Engineering, Yamaguchi University, Tokiwadai 2-16-1, Ube-shi, Yamaguchi 755-8611, Japan.
[2] Present address: Graduate School of Life Science and Systems Engineering, Kyushu Institute of Technology, Hibikino 2-4, Wakamatsu-ku, Kitakyushu 808-0196, Japan.

0020-1693/$ - see front matter © 2007 Elsevier B.V. All rights reserved.
doi:10.1016/j.ica.2006.12.036

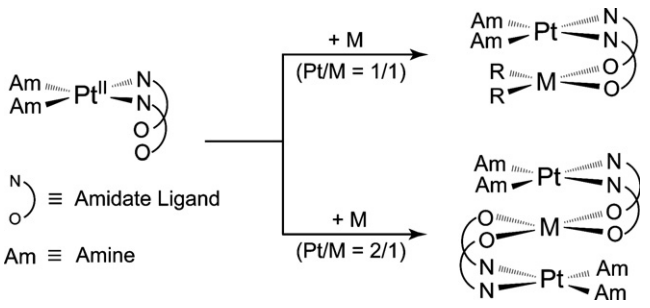

Scheme 1.

although the isomerization is known to occur at high temperature. The final amidate-hanging complex is readily obtainable in a pure form without further procedure to remove large excess of free amide ligand released during the reaction. In the early studies [14–20], those direct hydrolysis reaction on Pt complexes have been thoroughly investigated, however, systematic synthetic reports of the ''amidate-hanging'' Pt mononuclear complexes were only a few. Herein we report a systematic synthetic method for novel five ''amidate-hanging'' Pt mononuclear complexes, *cis*-[Pt(PVM)$_2$(en)] · 4H$_2$O (**1**), *cis*-[Pt(PVM)$_2$(NH$_2$CH$_3$)$_2$] · H$_2$O (**2**), *cis*-[Pt(PVM)$_2$(NH$_2$^{t}Bu)$_2$] (**3**), *cis*-[Pt(TCM)$_2$(NH$_3$)$_2$] (**4**), and *cis*-[Pt(BZM)$_2$(NH$_3$)$_2$] (**5**) (Scheme 2), which could be useful for the synthesis of Pt and heterometal multinuclear chain complexes. Discussion on the crystal packing of the compounds related to **1**–**5** and the results of the ^{195}Pt NMR spectroscopy of **1**–**5** are also included.

2. Experimental

2.1. Materials

Pivalonitrile and trichloroacetonitrile were obtained from Tokyo Kasei Industrial Co. AgClO$_4$ · H$_2$O, NH$_2$CH$_3$, and NH$_2$^{t}Bu were obtained from Kanto Chemical Co. NaOH and benzonitrile were obtained from Wako Co. K$_2$PtCl$_4$ was obtained from Tanaka Kikinzoku Co. CAUTION: The following preparations use AgClO$_4$, which is potentially explosive.

2.2. Synthesis of *cis*-[Pt(PVM)$_2$(en)] · 4H$_2$O (**1**)

An aqueous solution (40 mL) of *cis*-[Pt(en)I$_2$] (9.7 mmol, 4.94 g), which was prepared according to the reported procedure [21], was stirred with 2 equiv. of AgClO$_4$ · H$_2$O (19.4 mmol, 4.37 g) for 20 h in the dark, and AgI was then removed by filtration. The yellow filtrate was stirred with 2 equiv. of pivalonitrile (19.4 mmol, 2.12 mL) for 1 day. The resulting white powder, *cis*-[Pt(NCCMe$_3$)$_2$(en)](ClO$_4$)$_2$ (**P1**), was recrystallized by diffusing 2.0 equiv. NaOH solid to the aqueous (10 mL) solution, to obtain white powder (**1**). Yield 33%. Elemental *Anal.* Calc. for C$_{12}$H$_{36}$N$_4$O$_6$Pt: C, 27.32; H, 6.88; N, 10.62. Found: C, 27.97; H, 5.91; N, 10.71%.

2.3. Synthesis of *cis*-[Pt(PVM)$_2$(NH$_2$CH$_3$)$_2$] · H$_2$O (**2**)

cis-[Pt(NH$_2$CH$_3$)$_2$Cl$_2$] was obtained according to the procedure for analogous compounds [16]. An aqueous solution (50 mL) of *cis*-[Pt(NH$_2$CH$_3$)$_2$Cl$_2$] (13.0 mmol, 4.26 g) was stirred with 2 equiv. of AgClO$_4$ · H$_2$O (26.0 mmol, 5.86 g) for 19 h in the dark, and AgCl was then removed by filtration. The colorless filtrate was stirred with 2 equiv. of pivalonitrile (26.0 mmol, 2.84 mL) for 2 days. The resulting white powder, *cis*-[Pt(NCCMe$_3$)$_2$(NH$_2$CH$_3$)$_2$](ClO$_4$)$_2$ (**P2**), was recrystallized by diffusing 2.0 equiv. NaOH to the aqueous (20 mL) solution, to obtain white powder (**2**). Yield 52%. Elemental *Anal.* Calc. for C$_{12}$H$_{32}$N$_4$O$_3$Pt: C, 30.31; H, 6.78; N, 11.78. Found: C, 30.52; H, 6.17; N, 11.71%.

2.4. Synthesis of *cis*-[Pt(PVM)$_2$(NH$_2$^{t}Bu)$_2$] (**3**)

An aqueous solution (4 mL) of K$_2$PtCl$_4$ (1.0 mmol, 0.42 g) was stirred with 4 equiv. of KI (4.0 mmol, 0.66 g) for 15 min at 40 °C, and then 2 equiv. 30 w% NH$_2$^{t}Bu (2.0 mmol, 0.49 g) was added. After stirring for 20 min at

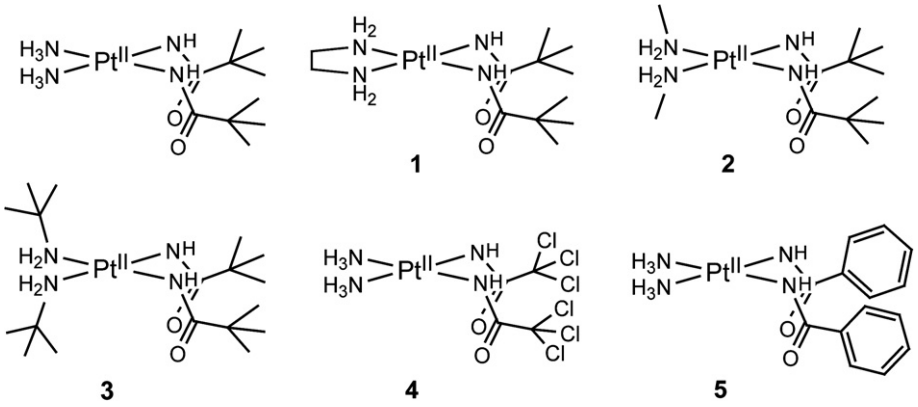

Scheme 2.

40°C, yellow powder was obtained. An aqueous solution (4 mL) of the yellow powder (0.60 g) was stirred with $AgClO_4 \cdot H_2O$ (2.0 mmol, 0.45 g) for 20 h in the dark, and AgCl was then removed by filtration. The colorless filtrate was stirred with pivalonitrile (2.0 mmol, 0.22 mL) for 3 h. The resulting white powder, *cis*-$[Pt(NCCMe_3)_2(NH_2{}^tBu)_2](ClO_4)_2$ (**P3**), was recrystallized by diffusing 2.0 equiv. NaOH to the aqueous (2 mL) solution, to obtain white powder (**3**). Yield 15%. Elemental *Anal.* Calc. for $C_{18}H_{42}N_4O_2Pt$: C, 39.92; H, 7.82; N, 10.34. Found: C, 39.86; H, 7.81; N, 10.18%. For single crystal X-ray analysis, *cis*-$[Pt(PVM)_2(NH_2{}^tBu)_2] \cdot MeOH$ (**3′**) was obtained by the recrystallization in MeOH solution.

2.5. Synthesis of cis-[Pt(TCM)$_2$(NH$_3$)$_2$] (4)

An aqueous solution (16 mL) of *cis*-$[Pt(NH_3)_2Cl_2]$ (4.0 mmol, 1.20 g) was stirred with 2 equiv. of $AgClO_4 \cdot H_2O$ (8.0 mmol, 1.80 g) for 18 h in the dark, and AgCl was then removed by filtration. The colorless filtrate was dried up and dissolved in 4.5 mL MeOH, and stirred with 2 equiv. of trichloroacetonitrile (8.0 mmol, 0.92 mL) for 14 h. The resulting white suspension was dried up to obtain the white product, $[Pt(TCM)(NH(C{=}OH)CCl_3)(NH_3)_2](ClO_4)$ (**P4**). The product was recrystallized by diffusing 2.0 equiv. NaOH to the aqueous (4 mL) solution of **P4**, to obtain white powder (**4**). Yield 55%. Elemental *Anal.* Calc. for $C_4H_8Cl_6N_4O_2Pt$: C, 8.70; H, 1.46; N, 10.15. Found: C, 8.78; H, 1.57; N, 9.81%. For single crystal X-ray analysis, *cis*-$[Pt(TCM)_2(NH_3)_2] \cdot MeOH$ (**4′**) was obtained by the recrystallization in MeOH solution.

2.6. Synthesis of cis-[Pt(BZM)$_2$(NH$_3$)$_2$] (5)

An aqueous solution (8 mL) of *cis*-$[Pt(NH_3)_2Cl_2]$ (4.0 mmol, 1.20 g) was stirred with 2 equiv. of $AgClO_4 \cdot H_2O$ (8.0 mmol, 1.80 g) for 30 h in the dark, and AgCl was then removed by filtration. The colorless filtrate was stirred with 2 equiv. of benzonitrile (8.0 mmol, 0.82 mL) for 1 day. The resulting white powder, *cis*-$[Pt(NCPh)_2(NH_3)_2](ClO_4)_2$ (**P5**), was recrystallized by diffusing 2.0 equiv. NaOH to the aqueous (20 mL) solution, to obtain white powder (**5**). Yield 49%. Elemental *Anal.* Calc. for $C_{14}H_{18}N_4O_2Pt$: C, 35.82; H, 3.87; N, 11.94. Found: C, 34.79; H, 3.85; N, 11.42%.

2.7. X-ray structure determination

Measurements were carried out on a Bruker SMART APEX CCD diffractometor equipped with a normal focus Mo-target X-ray tube ($\lambda = 0.71073$ Å) operated at 2000 W power (50 kV, 40 mA) and a CCD two-dimensional detector. A total of 1315 frames were collected with a scan width of 0.3° in ω with an exposure time of 20 (**1**), 20 (**3**), 20 (**P4**), 15 (**4**), 45 (**P5**), and 35 (**5**) s/frame. The frames were integrated with the SAINT software package with a narrow frame algorithm [22]. Absorption correction was applied by using SADABS [23]. All the structures were solved by the direct method with the subsequent difference Fourier syntheses and the refinement with the SHELXTL (version 5.1) software package [24]. The crystal data and the details of the structure determinations are summarized in Table 1. For all compounds, the non-hydrogen atoms were refined anisotropically and all hydrogen atoms were placed in the ideal positions. In **1**, highly disordered H_2O molecules (O5–12), C1–3, C11, C13, and C18 atoms were refined isotropically. In **4′**, N2 and C3 atoms were refined isotropically. In **P5**, benzene rings (C2–7 and C9–14) were isotropically refined under rigid condition. In **5**, C9 atom was refined isotropically.

3. Results and discussion

3.1. Synthesis, products, and ^{195}Pt NMR

Compounds **1**–**5** were obtained by direct base hydrolysis of the corresponding nitrile complexes as shown in Scheme 3. As mentioned in Section 2, the aqueous solutions of $[Pt(OH_2)_2(Am)_2](ClO_4)_2$ ($Am = NH_3$, NH_2CH_3, $NH_2{}^tBu$, $(Am)_2 =$ en) were obtained by the removal of halogen ions from *cis*-$[PtX_2(Am)_2]$ ($X = Cl^-$, I^-) with silver salts. Nitriles were successfully introduced into $[Pt(OH_2)_2(Am)_2](ClO_4)_2$ in H_2O to obtain white powders, *cis*-$[Pt(NCCMe_3)_2(en)](ClO_4)_2$ (**P1**), *cis*-$[Pt(NCCMe_3)_2(NH_2CH_3)_2](ClO_4)_2$ (**P2**), *cis*-$[Pt(NCCMe_3)_2(NH_2{}^tBu)_2](ClO_4)_2$ (**P3**), and *cis*-$[Pt(NCPh)_2(NH_3)_2](ClO_4)_2$ (**P5**) as the precursor complexes for **1**, **2**, **3**, and **5**, respectively. On the other hand, the reaction of $[Pt(OH_2)_2(NH_3)_2](ClO_4)_2$ and 2 equiv. trichloroacetonitrile in H_2O lead to the dinuclear complex, $[Pt_2(TCM)_2(NH_3)_4](ClO_4)_2$, since the N≡C moiety in trichloroacetonitrile more easily undergoes water nucleophilic attack than other nitriles [25]. In MeOH, this dimerization did not occur, and the mononuclear complex with mixed-ligands, $[Pt(TCM)(NH(C{=}OH)CCl_3)(NH_3)_2](ClO_4)$ (**P4**), was obtained as white powder.

All of the compounds **P1**–**5** were treated by base-hydrolysis to give the bisamidate *cis*-$[Pt(HNCOR)_2(Am)_2]$ (**1**: $R = {}^tBu$, $(Am)_2 =$ en; **2**: $R = {}^tBu$, $Am = NH_2CH_3$; **3**: $R = {}^tBu$, $Am = NH_2{}^tBu$; **4**: $R = CCl_3$, $Am = NH_3$; **5**: $R = Ph$, $Am = NH_3$), which were characterized by MS, ^{1}H NMR, and IR spectroscopy.[3] The IR spectra of **1**–**5** lack the CN stretching bands and show clearly the presence of amide-I bands; 1591 and 1556 (**1**), 1625 and 1545 (**2**), 1552 (**3**), 1662 (**4**), and 1597 cm^{-1} (**5**).

Subtle differences were observed in the ^{195}Pt NMR data, showing the differences of the Pt electron densities between **1**–**5**. The ^{195}Pt NMR chemical shifts obtained in MeOD by using an aqueous solution of $K_2[PtCl_6]$ as an external reference are −2692 (**1**), −2593 (**2**), −2599 (**3**), −2512 (**4**), and −2473 ppm (**5**) (Fig. 1), which are in the expected range for Pt(2+) complexes [25,26]. The ^{195}Pt NMR signals

[3] MS, ^{1}H NMR, and IR spectra are shown in supplementary material.

Table 1
Crystal data and structure refinement of $[Pt(PVM)_2(en)]\cdot 4H_2O$ (**1**), $[Pt(PVM)_2(NH_2{}^tBu)_2]\cdot MeOH$ (**3′**), $[Pt(TCM)(NH(C{=}OH)CCl_3)(NH_3)_2](ClO_4)$ (**P4**), $[Pt(TCM)_2(NH_3)_2]\cdot MeOH$ (**4′**), $[Pt(NCPh)_2(NH_3)_2](ClO_4)_2$ (**P5**), and $[Pt(BZM)_2(NH_3)_2]$ (**5**)

Compound	**1**	**3′**	**P4**	**4′**	**P5**	**5**
Chemical formula	$C_{24}H_{56}N_8O_{12}Pt_2$	$C_{19}H_{46}N_4O_3Pt$	$C_4H_8Cl_7N_4O_6Pt$	$C_5H_{11}Cl_6N_4O_3Pt$	$C_{14}H_{16}Cl_2N_4O_8Pt$	$C_{14}H_{18}N_4O_2Pt$
Formula weight	1038.95	573.69	651.38	582.97	634.30	469.41
Crystal system	triclinic	monoclinic	monoclinic	monoclinic	monoclinic	monoclinic
Space group	$P\bar{1}$	$P2_1/n$	$P2_1/n$	$P2_1/n$	$C2$	$P2_1/c$
Temperature (K)	120	120	120	120	120	120
Unit cell dimensions						
a (Å)	12.359(5)	11.080(3)	6.1429(12)	15.234(7)	25.016(6)	15.933(10)
b (Å)	13.270(6)	17.501(5)	35.252(7)	6.411(3)	8.2083(18)	5.854(4)
c (Å)	13.980(6)	13.248(4)	8.1764(16)	17.018(7)	9.620(2)	16.827(10)
α (°)	111.819(7)	90	90	90	90	90
β (°)	99.763(8)	98.935(5)	94.941(3)	92.441(8)	92.670(4)	94.528(12)
γ (°)	106.139(7)	90	90	90	90	90
V (Å^3)	1946.6(14)	2537.8(12)	1764.0(6)	1660.6(13)	1973.1(7)	1564.7(17)
Z	2	4	4	4	4	4
D_c (g cm^{-1})	1.773	1.502	2.453	2.332	2.135	1.993
μ (Mo Kα) (mm^{-1})	7.239	5.552	9.041	9.420	7.433	8.977
F(000)	1016	1160	1220	1092	1216	896
θ Range (°)	1.65–27.56	1.94–27.57	1.16–27.52	1.83–27.64	1.63–27.51	1.28–27.58
Goodness-of-fit on F^2	1.103	1.023	1.041	1.020	1.100	1.063
R_1,[a] wR_2[b] [$I > 2\delta(I)$]	0.1150, 0.3010	0.0416, 0.1005	0.0590, 0.1491	0.0984, 0.2188	0.0462, 0.1191	0.0711, 0.1719
R_1,[a] wR_2[b] (all data)	0.1458, 0.3215	0.0526, 0.1069	0.0779, 0.1608	0.1188, 0.2359	0.0579, 0.1389	0.0967, 0.1959

[a] $R = \sum \| F_o | - | F_c \| / \sum | F_o |$.

[b] $R_w = \left\{ \sum w \left[\left(F_o^2 - F_c^2 \right)^2 \right] / \left[\left(\sum w F_o^2 \right)^2 \right] \right\}^{1/2}$.

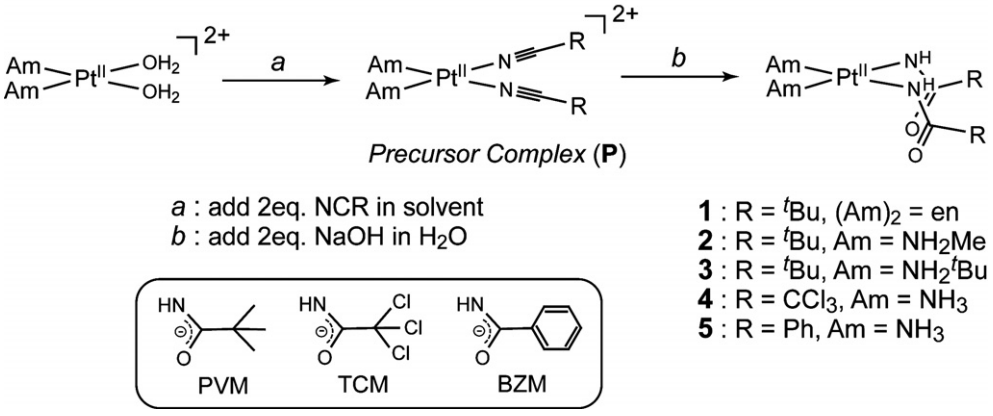

Scheme 3.

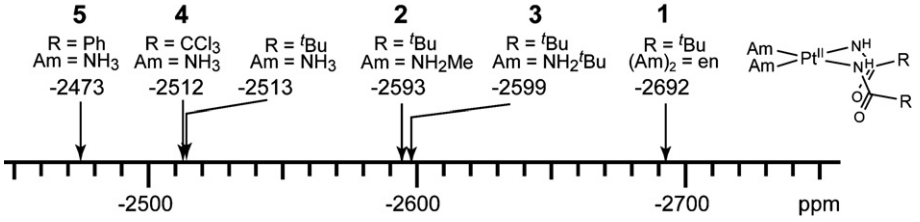

Fig. 1. ^{195}Pt chemical shifts of **1**–**5** in MeOH.

were broad, probably due to the coupling of the ^{195}Pt nuclear spin with the ^{14}N nuclear spins around it [26].

Whereas relatively small variation (<100 ppm) of the ^{195}Pt NMR chemical shift was observed between *cis*-$[Pt(PVM)_2(NH_3)_2]\cdot 2H_2O$, **4**, and **5**, the change of the chemical shift by substitution of the amine ligands was significantly large between *cis*-$[Pt(PVM)_2(NH_3)_2]\cdot 2H_2O$ [13] and **1**–**3**. More electron-donating substitution of R from H to CH_3, and ^{t}Bu in NH_2R induced marked upfield shift of the platinum signal. The signal in compound **1** was

150 ppm more upfield shifted than that in *cis*-$[Pt(PVM)_2(NH_3)_2]\cdot 2H_2O$. There is no clear suggestion relating these observations to chemical shift theory, but the tendency is similar to those observed in *cis*-$[PtCl_2(Am)_2]$ series; *cis*-$[PtCl_2(NH_3)_2]$ (−2097 ppm), *cis*-$[PtCl_2(NH_2Me)_2]$ (−2188 ppm), *cis*-$[PtCl_2(NH_2iPr)_2]$ (−2224 ppm), *cis*-$[PtCl_2(en)]$ (−2345 ppm) [27].

3.2. Crystal structures

The single crystals suitable for X-ray analysis, *cis*-$[Pt(PVM)_2(en)]\cdot 4H_2O$ (**1**), *cis*-$[Pt(PVM)_2(NH_2{}^tBu)_2]\cdot$MeOH (**3′**), $[Pt(TCM)(NH(C{=}OH)CCl_3)(NH_3)_2](ClO_4)$ (**P4**), *cis*-$[Pt(TCM)_2(NH_3)_2]\cdot$MeOH (**4′**), *cis*-$[Pt(NCPh)_2(NH_3)_2](ClO_4)_2$ (**P5**), and *cis*-$[Pt(BZM)_2(NH_3)_2]$ (**5**), were successfully obtained during the above synthesis or by the recrystallization in MeOH. Selected bond distances found in **1**, **3′**, **P4**, **4′**, **P5**, and **5** are listed in Table 2. The details of the molecular structures and the crystal packings will be shown.

3.3. Crystal structures of cis-$[Pt(PVM)_2(en)]\cdot 4H_2O$ (1)

Fig. 2a shows the crystal structure of compound **1**. Compound **1** has two individual mononuclear complexes in the unit cell. The square-planar coordination geometry around the Pt atom consists of two *cis* N atoms of ethylenediamine and two *cis* N atoms of PVM ligands. The sum of the four N–Pt–N angles is 360.0° and 360.1°, which is indicative of their co-planarity. As shown in Table 2, the C(3)═O(1) (1.28(3) Å) and C(8)═O(2) (1.24(4) Å) bond lengths are in agreement with a double-bond character and sp^2 hybridized the C and O atoms. On the other hand, the C(3)–N(3) (1.31(4) Å) and C(8)–N(4) (1.30(3) Å) are shorter than expected, indicating a partial double-bond character. The bond distances and angles are essentially the same as reported for *cis*-$[Pt(NH_3)_2(PVM)_2]\cdot 2H_2O$ [13]. The crystal is solvated and contains four highly disordered water molecules.

An interesting feature of the crystal packing is that two complex molecules stack in a face-to-face fashion with double intermolecular NH (en)–O (amide) hydrogen bonds,

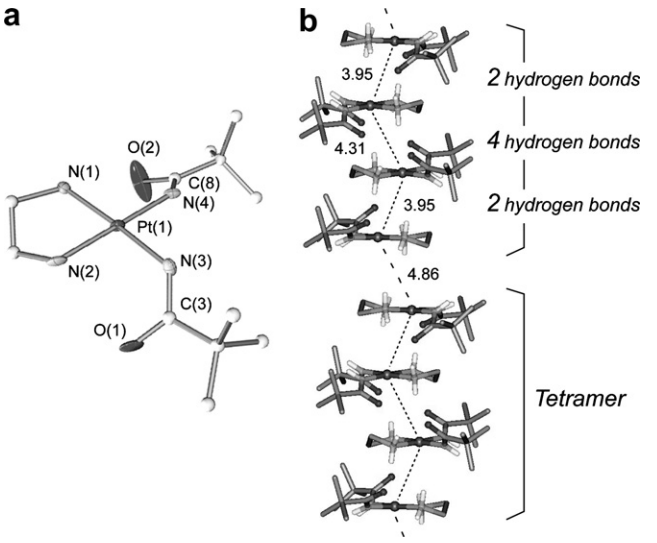

Fig. 2. (a) Crystal structure of $[Pt(PVM)_2(en)]\cdot 4H_2O$ (**1**). Hydrogen atoms and water molecules are omitted for clarity. (b) Crystal structure of **1**. Four molecules of the mononuclear complex are stabilized by intermolecular hydrogen bonds to form one-dimensional tetrametallic units.

where Pt–Pt distance is a relatively short (3.95 Å). Those dimeric units are stabilized with four hydrogen bonds between ethylenediamine and amidate moieties to afford tetrameric units (Fig. 2b). The tetrameric units are aligned in a quasi one-dimensional chain without significant interaction among them.

3.4. Crystal structures of cis-$[Pt(PVM)_2(NH_2{}^tBu)_2]\cdot$MeOH (3′)

Fig. 3 shows the crystal structure of **3′**. The Pt atom of **3′** is *cis* coordinated to two $NH_2{}^tBu$ and two PVM ligands with the Pt–N bond distances similar to **1** (Table 2). The amidate planes inclines by 39° and 62° with respect to the Pt coordination plane. Both *t*-butyl moieties in the $NH_2{}^tBu$ ligands are located in the upper side of the coordination plane, whereas those in the PVM ligands are located in the opposite side. One amidate moiety in the PVM ligand is hydrogen bonded to the $NH_2{}^tBu$ ligands (O(amide)

Table 2
Selected bond distances (Å) for **1**, **3′**, **P4**, **4′**, **P5**, and **5**

Compound	1[a]	3′	P4	4′	P5	5
Pt(1)–N(1)	2.06(2)	2.080(4)	2.056(10)	2.053(11)	2.132(13)	2.087(11)
Pt(1)–N(2)	2.01(2)	2.079(5)	2.031(10)	2.030(11)	2.038(7)	2.072(11)
Pt(1)–N(3)	2.00(2)	2.009(4)	2.011(10)	2.014(12)	1.881(12)	2.027(11)
Pt(1)–N(4)	1.97(2)	2.004(5)	2.039(9)	1.997(13)	1.975(8)	2.023(11)
C═O (amide)	1.28(3)	1.254(6)	1.240(14)	1.212(17)		1.287(17)
	1.24(4)	1.260(6)	1.326(14)	1.235(17)		1.267(16)
N–C (amide)	1.31(4)	1.311(7)	1.291(15)	1.299(17)	1.160(16)[b]	1.338(17)
	1.30(3)	1.323(7)	1.252(14)	1.316(18)	1.139(12)[b]	1.316(16)

[a] Compound **1** contains two crystallographically independent mononuclear complexes, and other distances are Pt(2)–N(5) = 2.00(2), Pt(2)–N(6) = 2.07(3), Pt(2)–N(7) = 1.99(2), Pt(2)–N(8) = 2.00(2), C═O (amidate) = 1.27(3) and 1.30(3), and N–C (amidate) = 1.32(4) and 1.32(3) Å.
[b] N≡C distance.

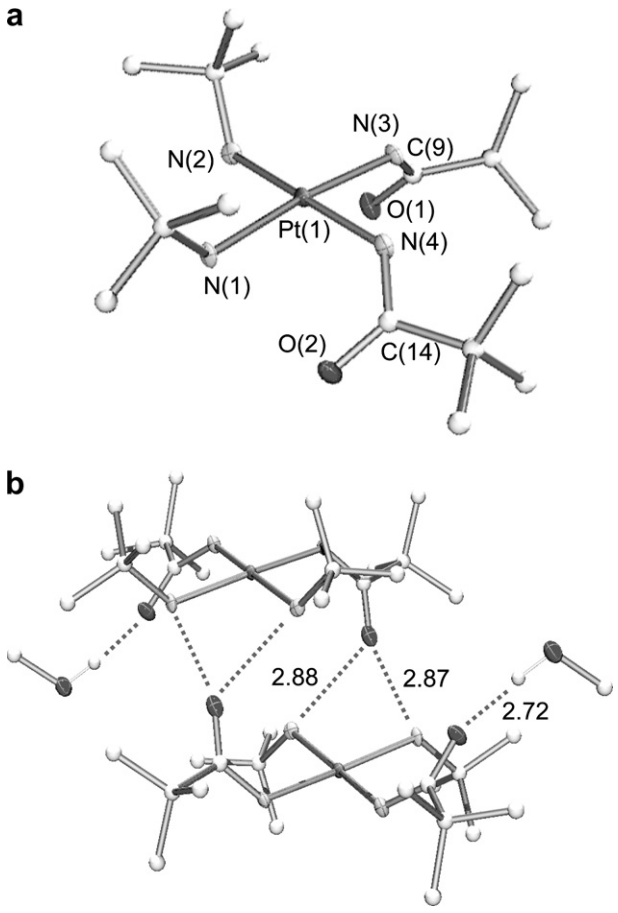

Fig. 3. (a) Crystal structure of $[Pt(PVM)_2(NH_2{}^tBu)_2]\cdot MeOH$ (**3′**). Hydrogen atoms are omitted for clarity. (b) Two mononuclear **3′** are dimerized with four intermolecular hydrogen bonds.

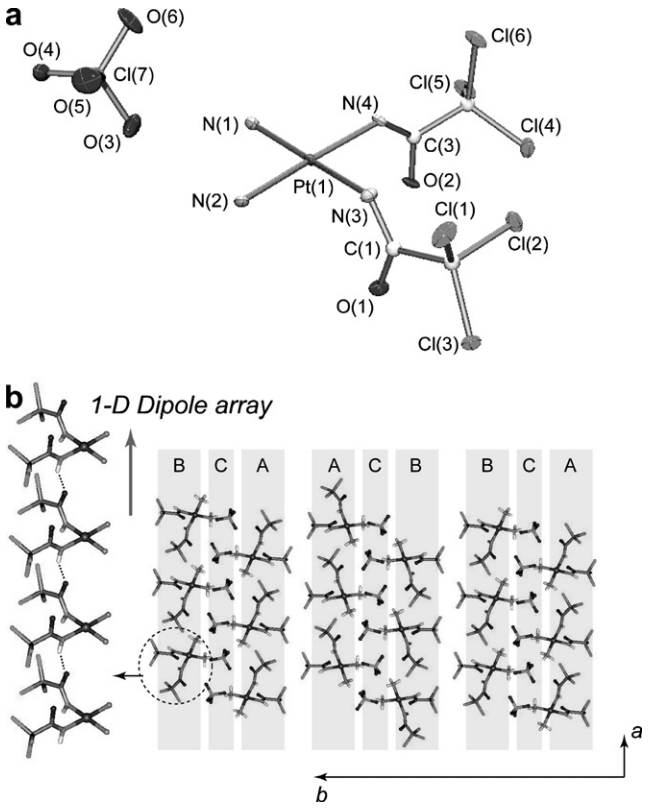

Fig. 4. (a) Crystal structure of $[Pt(TCM)(NH(C{=}OH)CCl_3)(NH_3)_2](ClO_4)$ (**P4**). Hydrogen atoms are omitted for clarity. (b) Crystal packing of **P4**. Platinum mononuclear complexes are stacked along the *c*-axis to afford one-dimensional dipole array attributed to amidate–amidate hydrogen bonds.

–N($NH_2{}^tBu$) = 2.87, 2.88 Å) in the neighboring molecule, and another is hydrogen bonded to a MeOH molecule (O(amide)–O(MeOH) = 2.72 Å). Since PVM ligands have both hydrogen-donor and -acceptor sites, congested hydrogen bonding network is formed in this case, and the Pt mononuclear complexes are dimerized as shown in Fig. 3b.

3.5. Crystal structures of $[Pt(TCM)(NH(C{=}OH)CCl_3)(NH_3)_2](ClO_4)$ (P4) and cis-$[Pt(TCM)_2(NH_3)_2]\cdot MeOH$ (4′)

Fig. 4 shows the crystal structure of **P4**. The Pt atom of **P4** is also *cis* coordinated to four *N*-donor ligands with similar distances to **1** and **3′** (Table 2). Most remarkable feature of **P4** is that it comprises the mixed-ligands, $NH(C{=}O)CCl_3$ and $NH(C{=}OH)CCl_3$. The X-ray analysis surely exhibits a significant difference among the C=O distances; C(1)=O(1) = 1.240(14) and C(3)–O(2) = 1.326(14) Å. Considering the electronic charge balance to ClO_4^- anion in the **P4** crystal, a H^+ ion must exist around the O(2) atom, although the position was not determined by X-ray analysis. The Pt mononuclear complexes are stacked along the *c*-axis, where amidate–amidate hydrogen bonds are effectively formed; N(amidate)–O(amidate) = 2.83 Å (Fig. 4b). These amidate–amidate hydrogen bonds afford one-dimensional dipole arrays along the *c*-axis, forming dipole columns. The dipole columns are aligned to create sheets (A and B), in which all dipole arrays are directed to the same direction. The sheets A and B are juxtaposed with the repetition, –A–C–B–B–C–A–, including ClO_4^- anions (C), and thus the dipole moments are cancelled out.

Fig. 5 shows the crystal structure of **4′**. The Pt atom of **4′** is also *cis* coordinated to four *N*-donor ligands. The C(1)–O(1) (1.212(17) Å) and C(3)–O(2) (1.235(17) Å) bond lengths are in agreement with a double-bond character and sp^2 hybridized C and O atoms. Thus, X-ray analysis also reveals that base hydrolysis of **P4** is completed without the geometry isomerization. Both amidate planes are perpendicular to the Pt coordination plane, and the carbonyl moieties are hydrogen bonded to the neighboring NH_3 ligands to form the one-dimensional column along the *b*-axis. The columns are aligned in parallel, and methanol molecules fill the cavities among the columns as guest molecules.

3.6. Crystal structures of cis-$[Pt(NCPh)_2(NH_3)_2](ClO_4)_2$ (P5) and cis-$[Pt(BZM)_2(NH_3)_2]$ (5)

Fig. 6 shows the crystal structures of **P5** and **5**. In both **P5** and **5**, the Pt atom is also *cis* coordinated to four *N*-donor ligands. In **P5**, the benzonitrile ligands are almost

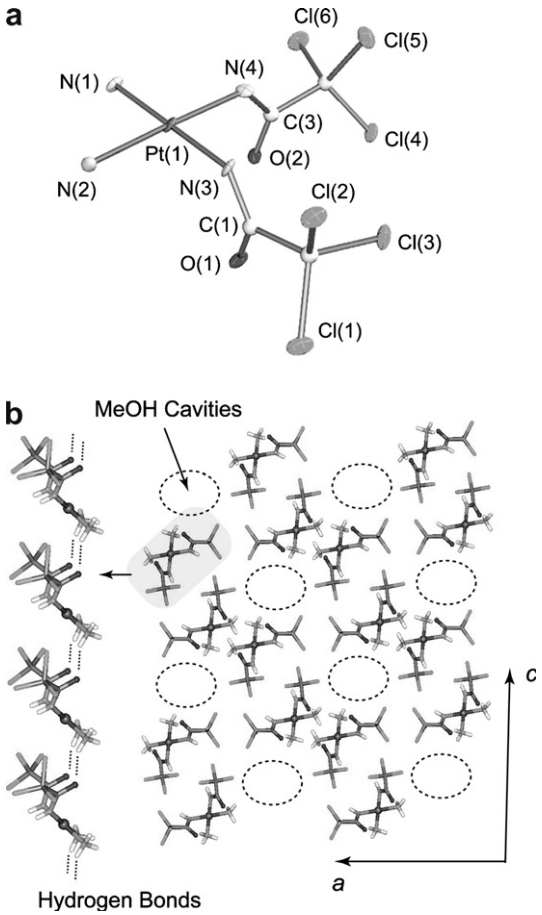

Fig. 5. (a) Crystal structure of $[Pt(TCM)_2(NH_3)_2] \cdot MeOH$ (**4′**). Hydrogen atoms and MeOH molecules are omitted for clarity. (b) Crystal packing of **4′**. Platinum mononuclear complexes are stacked along the *b*-axis, where cavities fulfilled with MeOH molecules are formed.

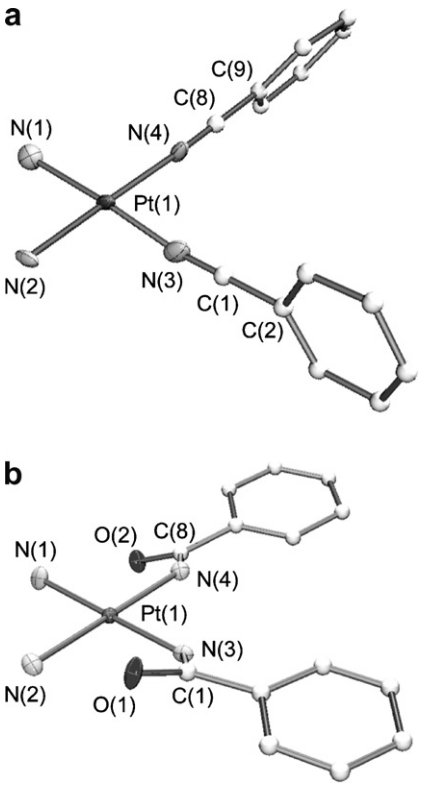

Fig. 6. (a) Crystal structure of $[Pt(NCPh)_2(NH_3)_2](ClO_4)_2$ (**P5**). Hydrogen atoms and ClO_4^- molecules are omitted for clarity. (b) Crystal structure of $[Pt(BZM)_2(NH_3)_2]$ (**5**). Hydrogen atoms are omitted for clarity.

linear (N(3)–C(1)–C(2) = 179.9(16)° and N(4)–C(8)–C(9) = 178.9(16)°) and are bound to the Pt atom through the electron lone pair on the nitrogen atom with the coordination angles Pt(1)–N(3)–C(1) = 171.7(12)° and Pt(1)–N(4)–C(8) = 174.1(17)°. Such slightly bent M–N–C moieties are also observed in other metal nitrile complexes and are attributed to a partial sp^2 character of the donor nitrogen atom [16]. The Pt–N bond lengths are in good agreement with those in other Pt nitrile complexes.

Compound **5** is obtained by the base hydrolysis of **P5**. No ClO_4^- anion and water molecule is incorporated in the crystal lattice, showing completion of the base hydrolysis. As shown in Table 2, the C(1)=O(1) (1.287(17) Å) and C(8)=O(2) (1.267(16) Å) bond lengths are in agreement with a double-bond character and sp^2 hybridized C and O atoms. Amidate planes tilt to both the Pt coordination planes (28.1° and 33.3°) and benzene rings (29.3° and 26.5°).

In summary, the present work established the synthesis of five "amidate-hanging" Pt mononuclear complexes, which were synthesized by conversion of the Pt-bound nitrile into amidate. As confirmed by X-ray diffraction analysis, the *cis* geometry of the PtN_4 coordination in the Pt mononuclear complexes is maintained during the conversion. The ^{195}Pt NMR measurement showed subtle difference of the Pt electronic densities between **1**–**5**. Using amidate-hanging Pt mononuclear complexes described here, attempts to prepare new hetero-metal chain complexes composed of Pt–M and Pt–M–Pt, are currently in progress.

Acknowledgements

This work was supported by the Iketani Science and Technology Foundation, Grants-in-Aid for Scientific Research (Young Scientist (B) No. 17750058), and the 21COE program "Practical Nano-Chemistry" from MEXT, Japan.

Appendix A. Supplementary material

CCDC 624151, 624152, 624153, 624154, 624155 and 624156 contain the supplementary crystallographic data for **1**, **3′**, **P4**, **4′**, **P5** and **5**. These data can be obtained free of charge via http://www.ccdc.cam.ac.uk/conts/retrieving.html, or from the Cambridge Crystallographic Data Centre, 12 Union Road, Cambridge CB2 1EZ, UK; fax: (+44) 1223-336-033; or e-mail: deposit@ccdc.cam.ac.uk. Supplementary data associated with this article can be found, in the online version, at doi:10.1016/j.ica.2006.12.036.

References

[1] F.A. Cotton, L.R. Falvello, R. Uson, J. Fornies, M. Tomas, J.M. Casas, I. Ara, Inorg. Chem. 26 (1987) 1366.
[2] T. Yamaguchi, F. Yamazaki, T. Ito, J. Am. Chem. Soc. 121 (1999) 7405.
[3] T. Yamaguchi, F. Yamazaki, T. Ito, J. Am. Chem. Soc. 123 (2001) 743.
[4] W. Micklitz, G. Miiller, B. Huber, J. Riede, F. Rashwan, J. Heinze, B. Lippert, J. Am. Chem. Soc. 110 (1988) 7084.
[5] E. Zangrando, F. Pichierri, L. Randaccio, B. Lippert, Coord. Chem. Rev. 156 (1996) 275.
[6] B. Lippert, Coord. Chem. Rev. 182 (1999) 263.
[7] W. Chen, F. Liu, T. Nishioka, K. Matsumoto, Eur. J. Inorg. Chem. (2003) 4234.
[8] W. Chen, F. Liu, K. Matsumoto, J. Autschbach, B.L. Guennic, T. Ziegler, M. Maliarik, J. Glaser, Inorg. Chem. 45 (2006) 4526.
[9] W. Chen, F. Liu, D. Xu, K. Matsumoto, S. Kishi, M. Kato, Inorg. Chem. 45 (2006) 5552.
[10] K. Uemura, K. Yamasaki, K. Fukui, K. Matsumoto, Eur. J. Inorg. Chem., in press.
[11] K. Uemura, K. Fukui, H. Nishikawa, S. Arai, K. Matsumoto, H. Oshio, Angew. Chem., Int. Ed. 44 (2005) 5459.
[12] K. Uemura, K. Fukui, K. Yamasaki, K. Matsumoto, Sci. Tech. Adv. Mater. 7 (2006) 461.
[13] W. Chen, K. Matsumoto, Inorg. Chim. Acta 342 (2003) 88.
[14] L. Maresca, G. Natile, F.P. Intini, F. Gasparrini, A. Tiripicchio, M. Tiripicchio-Camellini, J. Am. Chem. Soc. 108 (1986) 1180.
[15] R. Cini, F.P. Fanizzi, F.P. Intini, L. Maresca, G. Natile, J. Am. Chem. Soc. 115 (1993) 5123.
[16] A. Erxleben, I. Mutikainen, B. Lippert, J. Chem. Soc., Dalton Trans. (1994) 3667.
[17] R. Cini, P.A. Caputo, F.P. Intini, G. Natile, Inorg. Chem. 34 (1995) 1130.
[18] A. Erxleben, B. Lippert, J. Chem. Soc., Dalton Trans. (1996) 2329.
[19] R. Cini, F.P. Fanizzi, F.P. Intini, C. Pacifico, G. Natile, Inorg. Chim. Acta 264 (1997) 279.
[20] R. Cini, A. Cavaglioni, F.P. Intini, F.P. Fanizzi, C. Pacifico, G. Natile, Polyhedron 18 (1999) 1836.
[21] M.J. Arendse, G.K. Anderson, N.P. Rath, Inorg. Chem. 38 (1999) 5864.
[22] SMART & SAINT Software Pakage, ver. 5.625, Siemens Energy & Automation, Inc., Analytical Instrumentation, Madison, WI, 2001.
[23] G.M. Sheldrick, SADABS, Software for Empirical Absorption Corrections, University of Göttingen, Germany, 1996.
[24] SHELXTL Reference Manual, ver. 5.1, Bruker AXS, Analytical X-ray Systems, Madison, WI, 1997.
[25] K. Uemura, K. Matsumoto, unpublished results.
[26] P.S. Pregosin, Coord. Chem. Rev. 44 (1982) 247.
[27] E. Gabano, E. Marengo, M. Bobba, E. Robotti, C. Cassino, M. Botta, D. Osella, Coord. Chem. Rev. 250 (2006) 2158, and references therein.